Noname manuscript No.
(will be inserted by the editor)

Feynman diagrams

From complexity to simplicity and back

Robert Harlander

Received: date / Accepted: date

Abstract The way from the path integral to Feynman diagrams is sketched. The emphasis is put on the decrease of complexity in this process, from infinite-dimensional integrals down to the apparent simplicity of child's play. On the other hand, also the subsequent increase in complexity when using Feynman diagrams to make realistic physical predictions is described, thus illustrating the dialectic between the simplicity and clarity of Feynman diagrams, and the complexity in their practical applications.

Keywords Feynman diagrams · Path integrals · Complexity · Simplicity

1 Introduction

Feynman diagrams are part of the theoretical toolbox of quantum field theory (QFT) which, loosely speaking, is the relativistic generalization of quantum mechanics. The intricacies of the latter have been a subject of the philosophical debate since its very conception at the beginning of the twentieth century [1]. With QFT, a number of additional conceptual problems arise, mostly related to mathematical consistency (see Ref. [2] for details). In this article though, we will leave most of these issues aside and focus on a very specific topic, related to the complexity of QFT when it is used to compare a specific particle model

This work was supported by *Deutsche Forschungsgemeinschaft*, projects HA 2990/7-2 and HA 2990/8-2 of the Research Unit "The Epistemology of the Large Hadron Collider" (FOR 2063), project nos. 286101044 and 234743567.

R. Harlander
TTK, RWTH Aachen University
Tel.: +49-241-80-27045
Fax: +49-241-80-22187
E-mail: harlander@physik.rwth-aachen.de

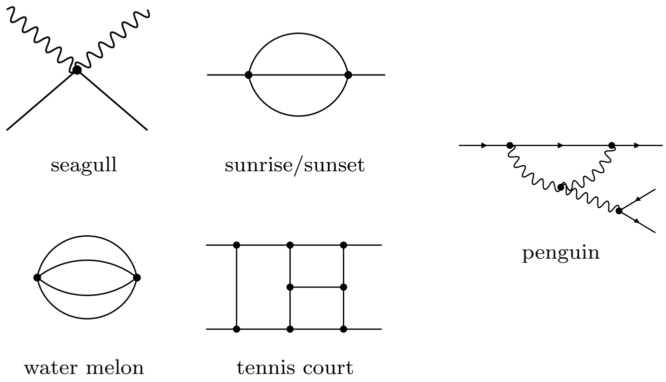

Fig. 1 A number of Feynman diagrams that have been given names by physicists. The origin of the "penguin" may be obscure; for the reader's amusement, we recommend to research the story behind it.

to experimental data.[1] But neither do we aim at evaluating the complexity of QFT as a theory itself, for example by comparing it to possible rival theories. Rather, we take QFT as given, and follow the steps it takes to bring it into quantitative contact with observation. This will illustrate the enormous simplification induced by Feynman diagrams when extracting physical information from a particle model. It culminates in the crystallization of Feynman diagrams as a stand-alone theoretical device which is no longer *applied* to QFT, but *encodes* it, albeit only in the perturbative limit. In the end, we will see how complexity creeps in again though, through the quest for precision.

Feynman diagrams have been indispensable for particle physics for about half a century now. Their historical development and dissemination as well as their diverse fields of application (calculation, communication, education, intuition, etc.) have been subject of study also in the reflective sciences [4–10]. And their multifaceted forms have inspired physicists even in non-scientific aspects, as exemplified by the creative names that they have given to specific diagrams, some of which are shown in Fig. 1.

In order to be able to appreciate the degree of simplification effectuated by Feynman diagrams, it will be helpful to first discuss the path integral formulation of QFT in Section 2. It helps to illustrate the intrinsic complexity of this theory, both from a pragmatic and an epistemic point of view (we adopt these notions from Ref. [11] throughout this paper). In Sections 3 and 4, we will see how Feynman diagrams facilitate the actual application of QFT to the calculation of physical quantities like cross sections. One of their main virtues, however, is that they largely detach this task from the original formalism. First and foremost, this implicates a drastic reduction in pragmatic

[1] Without alluding to the model/theory debate [3], we will adopt the term *particle model* for a specific, QFT-based model (or theory) of particle interactions, such as the Standard Model or its supersymmetric generalizations.

complexity when applying QFT. A large fraction of the operations required to get from the Lagrangian of a particular particle model to a cross section becomes *algorithmic*, meaning that they can be performed by a computer. Given the appropriate software, the calculation thus reduces to “pressing a button”, which is arguably the highest level of simplification that can be achieved. In fact, throughout most of this article, complexity (or simplicity) will be defined from this algorithmic point of view: A problem is considered simple if it requires little intellectual efforts to solve it [11].

Applying QFT in this purely algorithmic way reduces it to a black box at the cost of losing insight into the underlying physics. On the other hand, we suggest in Section 5 that the visual aspect of Feynman diagrams implies a significant *epistemic* simplification, since they lift the QFT description of a scattering to the level of a visual “experience”. After all, visualizability contributes to the virtues of a good scientific theory (see Ref. [12] for a recent review of theoretical virtues). Similar to Ref. [13], we will argue that it is irrelevant in this respect whether the image of a Feynman diagram truthfully represents the details of a physical process or not.

This article cannot provide a comprehensive introduction to path integrals or Feynman diagrams. We restrict ourselves to a rather schematic presentation of those aspects which are necessary to illustrate the main concern of this article pointed out above: How starting with a tremendously complex picture of the world, where the simple movement of a particle from one point in space to the other depends on the conditions at any other point in the universe, one arrives at stand-alone rules whose simplicity is close to that of child’s play, and whose representativeness can be both useful and deceiving [14].

Once this “metamorphosis” from quantum fields to Feynman diagrams is complete, we will look in Section 6 at the price that we have to pay for it, and what we need to do in order to settle the debts this has incurred. Feynman diagrams are based on perturbation theory, which is an approximation to the original path integral. Comparison to experimental results at high precision requires calculations at higher orders in perturbation theory, which re-introduces complexity in the Feynman diagrammatic approach. So far, it has paid off though: Particle physics has been enormously successful over the past few decades, and there is no question that Feynman diagrams played a major role in this.

Present-day perturbative calculations are computationally very intensive due to the sheer number of Feynman diagrams involved, leading to a large number of integrals, and the complexity of each of these integrals. In Section 7, we briefly sketch the workflow for a modern calculation in perturbation theory, with a particular focus on the current role of the visual aspect of Feynman diagrams.

We close our discussion with a few thoughts on the future of Feynman diagrams in Section 8.

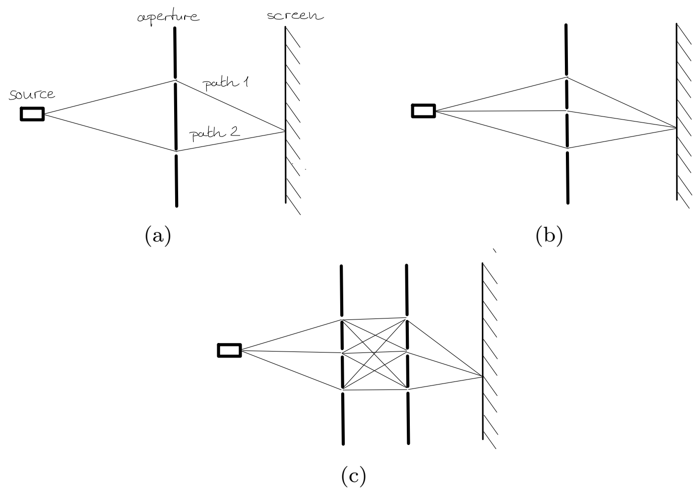

Fig. 2 (a) Double slit; (b) triple slit; (c) two triple slit apertures.

2 The path integral

There are essentially two ways to derive Feynman diagrams. In a typical physics curriculum, it is common to follow *canonical quantization* by default, which corresponds to generalizing the canonical quantum mechanical commutation relation $[x, p] = i\hbar$ to field theory. Here, however, we will consider the historically more appropriate and also more elegant approach via the path integral [15–17] (historical investigations on Feynman's lines of reasoning can be found in Refs. [9, 14], for example). This may seem very ambitious; after all, as opposed to the canonical commutation relation, the path integral is not necessarily a part of a regular quantum mechanics course. Nevertheless, once one engages with it, it provides a very helpful view on quantum mechanics, and allows for an enlightening transition to classical mechanics.

2.1 Definition of the path integral

In order to understand what the path integral is, let us recall the double slit experiment, see Fig. 2 (a). It consists of a source of particles (electrons, for example), a screen which detects them (like the screen of an old tube TV), and in between a double slit aperture. Classically, the electrons that traverse the aperture either pass through one slit or the other; their impacts on the screen will form two clusters, corresponding to the images of the two slits. In quantum mechanics, given suitable geometric dimensions of the aperture, the impacts on the screen form a more complex pattern. It resembles the interference pattern which would be caused by a laser beam of wavelength $\lambda = E/h$ traversing the aperture, where E is the energy of the electrons (including their relativistic rest energy $E_0 = mc^2$), and h is Planck's quantum of action. Usually, this behavior of the electrons is interpreted as them having wave character, and the interference pattern can be calculated accordingly, using the classical laws of optics. The calculated interference pattern reflects the probability distribution for a single electron to end up at a particular position on the screen.

The same probability distribution follows from the path integral formalism, however. It is proportional to the square of the *probability amplitude*,

$$\mathcal{A} \sim \sum_{\vec{x}} \exp\left(\frac{i}{\hbar} S[\vec{x}]\right) , \tag{1}$$

where $\exp(x) \equiv e^x$, the reduced Planck constant is $\hbar = h/(2\pi)$, and $S[\vec{x}]$ is the action for a path $\vec{x}$ that leads from the particle source to a particular position on the screen. The sum runs over *all paths*. In the case of the double slit experiment, to a good approximation one may take into account only the two paths which form a straight line from the source to one of the two slits, and from there to some point on the screen, see Fig. 2.

Let us now use a triple-slit aperture: clearly, the number of relevant paths increases to three in this case, see Fig. 2 (b). Of course, with every slit we add to the aperture, the number of paths increases. Similarly, we could include additional apertures, each of which has a certain number of slits, see e.g. Fig. 2 (c). So in the limit of infinitely many slits and apertures, we have to take into account infinitely many paths—but at some point, all the apertures will only consist of slits. The actual apertures are gone, but we still need to take into account infinitely many paths [18]! The collection of these paths densely fills all of space. Since each infinitesimal deformation of one path leads to another path, these paths cannot even be enumerated—they are uncountably infinitely many. In regular analysis, when going from discrete to continuous sets, we replace sums by integrals, and we do the same here:

$$\sum_{\vec{x}} \exp\left(\frac{i}{\hbar} S[\vec{x}]\right) \to \int \mathcal{D}\vec{x} \, \exp\left(\frac{i}{\hbar} S[\vec{x}]\right) . \tag{2}$$

Using the symbol $\mathcal{D}\vec{x}$ instead of $\mathrm{d}\vec{x}$ reminds us that the "integration variable" $\vec{x}$ is not a single point, but a whole *path* in space.[2]

Of course, if we consider several particles, the number of integration variables increases accordingly—which is not really a true complication, because this number is already infinite:

$$\int \mathcal{D}\vec{x}_1 \cdots \int \mathcal{D}\vec{x}_N \, \exp\left(\frac{i}{\hbar} S[\vec{x}_1, \ldots, \vec{x}_N]\right) . \tag{3}$$

[2] Let us briefly mention the bridge to classical physics at this point. It can be shown that, in the limit $\hbar \to 0$, the path integral is exhausted by the path which pertains to the minimum of the action. This is exactly the postulate of the *least-action principle* which determines the classical path of the particle. Note that, from this point of view, classical physics appears to have quite a singular character, since it singles out one path from an infinite, densely distributed set.

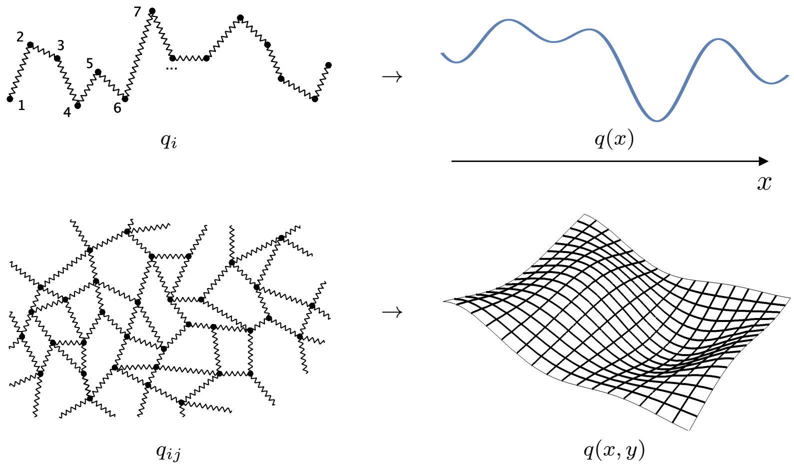

Fig. 3 Transition from discrete point mechanics to field theory in the one- and two-dimensional case.

Even the thermodynamic limit of infinitely many particles follows as a rather straightforward generalization of the N-particle case, formally obtained by adding a "$\lim_{N\to\infty}$" in front of Eq. (3).

The transition to field theory, however, truly brings in another level of complexity, because it replaces a discrete set of point particles by a continuous system. It is the same situation as replacing a chain of discrete masses connected to each other by massless springs by a continuous string, see Fig. 3. In the former case, one may label the displacement q_i of each mass from its equilibrium position by discrete indices $i = 1, 2, 3, \ldots$. For the string, however, we need a *field* $q(x)$, where $x \in [0, L]$ indicates a particular point along the string. So in the transition to field theory, the product of discrete path variable differentials $\mathcal{D}\vec{x}_i$ should be replaced by the product over the elements of a continuous set. Since there is not even a proper mathematical notation for this,[3] one simply writes

$$\int \mathcal{D}q \exp\left(\frac{i}{\hbar} S[q]\right) , \tag{4}$$

which *looks* identical to the path integral for a point particle of Eq. (3). However, it involves uncountably many times more integration variables, namely the value of the field q at each space-time point x.

[3] Just like there is no symbol for multiplying all real numbers within, say, the interval $(0, 1)$.

2.2 Solving the path integral

At first, this expression may look hopeless: how can we ever perform a literally uncountable (times uncountable!) number of integrals? But then again: in mathematics, dealing with infinite sets, infinite sums, or infinities in general is quite common. For example, it is a well-defined operation to add up infinitely many, albeit countable terms in a series such as $1+1/4+1/9+1/16+\cdots = \pi^2/6$. Summing up an uncountable number of terms is what we call an integral: $\int_0^1 \mathrm{d}x\, x = 1/2$. In a similar way, one can make sense out of the path integral. The situation is analogous to the historical development of calculus or distribution theory, where requirements from physics laid the foundation for new mathematical concepts.

One way to evaluate the path integral is through Gauß' integral:

$$\int_{-\infty}^{\infty} \mathrm{d}x \, \exp\left(-\frac{1}{2}ax^2\right) = \sqrt{\frac{2\pi}{a}}\,, \tag{5}$$

for arbitrary complex-valued a. Taking the derivative w.r.t. a on both sides, one finds

$$\begin{aligned} \int_{-\infty}^{\infty} \mathrm{d}x\, x^2 \, \exp\left(-\frac{1}{2}ax^2\right) &= a^{-1}\sqrt{\frac{2\pi}{a}}\,, \\ \int_{-\infty}^{\infty} \mathrm{d}x\, x^4 \, \exp\left(-\frac{1}{2}ax^2\right) &= 3\, a^{-2}\sqrt{\frac{2\pi}{a}}\,. \end{aligned} \tag{6}$$

Higher (even) powers of x in the integrand on the l.h.s. lead to higher inverse powers of a on the r.h.s.; integrals with odd powers of x vanish due to the $x \to -x$ asymmetry of the integrand.

The crucial point now is that these formulas can be generalized to arbitrary dimensions in a straightforward way. With a bit of basic linear algebra and some standard integration rules, one may show:

$$\begin{aligned} \int \mathrm{d}^n\vec{x}\, \exp\left(-\frac{1}{2}\vec{x}^T A\vec{x}\right) &= \sqrt{\frac{(2\pi)^n}{\det A}} \equiv \mathcal{N}\,, \\ \int \mathrm{d}^n\vec{x}\, x_i x_j \exp\left(-\frac{1}{2}\vec{x}^T A\vec{x}\right) &= \mathcal{N}\, A^{-1}_{ij}\,, \\ \int \mathrm{d}^n\vec{x}\, x_i x_j x_k x_l \exp\left(-\frac{1}{2}\vec{x}^T A\vec{x}\right) &= \mathcal{N}\, \left[A^{-1}_{ij}A^{-1}_{kl} + A^{-1}_{ik}A^{-1}_{jl} + A^{-1}_{il}A^{-1}_{jk}\right]\,, \end{aligned} \tag{7}$$

where $\vec{x}$ is an n-dimensional vector (not yet a path!) with elements $x_1, \ldots, x_n$, $\vec{x}^T$ is its transposed, A is an $n \times n$ matrix with elements $A_{11}, A_{12}, \ldots, A_{nn}$, $\det A$ is its determinant, and A^{-1} its inverse. The mathematics behind it is material of undergraduate physics. Note that Eqs. (5) and (6) follow for the special case $n = 1$, where we can set $x_1 = x$ and $A = a$.

But even readers who are *not* familiar with the underlying mathematics may recognize that the right-hand sides of Eq. (7) can be pictured as in Fig. 4.

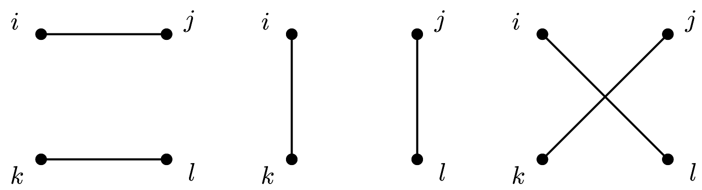

Fig. 4 Graphical representation of the terms in the last line of Eq. (7).

Each line in that figure corresponds to a factor A^{-1}, with the end points of that line matching the indices. Thus, each term in the last line of Eq. (7) is represented by one of the three *diagrams* in Fig. 4.

We have seen that these formulas are valid for arbitrary dimensions n. For the path integral, we need to consider the case of an infinite number of dimensions. One problem here is that $(\sqrt{2\pi})^n \to \infty$ for $n \to \infty$, so this limit cannot be taken in Eq. (7). Note, however, that in quantum physics we want to evaluate probabilities, and they are always normalized to one. This means that the integrals should be normalized as

$$\langle x_i x_j \cdots \rangle \equiv \frac{1}{\mathcal{N}} \int \mathrm{d}^n\vec{x}\, x_i x_j \cdots \exp\left(-\frac{1}{2}\vec{x}^T A\vec{x}\right) , \tag{8}$$

where the n-dependent factor $\mathcal{N}$ drops out, and the limit $n \to \infty$ can be taken, provided that the matrix A is invertible.[4]

All of these considerations are based on the fact that the argument of $\exp(\ldots)$ is quadratic in the integration variables. How is this helpful for a general action $S[\varphi]$? It so happens that any free action of relevance in our description of nature is indeed quadratic in the fields. "Free" here means that it describes fields/particles which do not interact with anything. Physically speaking, this is a completely academic case, because anything that does not interact does not leave a trace anywhere. From the point of view of a physicist, it may equally well not exist at all. Nevertheless, sometimes it is good to study academic cases, because it may help to bridge the gap to the real world. We will see how this happens in a bit.

The action for a free field $\varphi(x)$ may be written schematically as

$$S_{\text{free}}[\varphi] = -\frac{1}{2} \int \mathrm{d}^4x\, \varphi(x) D_x \varphi(x) , \tag{9}$$

where D_x is a differential operator whose specific form depends on the mass and spin of the particle under consideration. The only important thing at this point though is that we can consider D_x as an infinite-dimensional invertible

[4] Which it is, albeit only after "gauge fixing" in theories like quantum electrodynamics or the Standard Model.

matrix. For example, for a spin-0 field of mass m, it is

$$D_x^{-1} \equiv D^{-1}(x) = \int \frac{\mathrm{d}^4 p}{(2\pi)^4} e^{ip\cdot x} \tilde{D}^{-1}(p) \,, \qquad \tilde{D}^{-1}(p) = \frac{i}{p^2 - m^2} \,. \tag{10}$$

Here and in the following, we adopt *natural units*, i.e. we set $\hbar = c = 1$. The function D^{-1} and its Fourier transform $\tilde{D}^{-1}$ are called the *propagator* of the field φ in position and in momentum space, respectively.[5]

3 Scattering amplitudes and perturbation theory

The probability amplitude for two particles φ starting at space-time points x_1 and x_2 to evolve to x_3 and x_4 is given by the so-called *four-point function*

$$\begin{aligned} \langle \varphi_1 \varphi_2 \varphi_3 \varphi_4 \rangle &\equiv \frac{1}{\mathcal{N}} \int \mathcal{D}\varphi \, \varphi_1 \varphi_2 \varphi_3 \varphi_4 \, \exp\left(iS[\varphi]\right) \\ &\overset{S=S_{\text{free}}}{=} D_{12}^{-1} D_{34}^{-1} + D_{13}^{-1} D_{24}^{-1} + D_{14}^{-1} D_{23}^{-1} \,, \end{aligned} \tag{11}$$

where we used the short-hand notation $\varphi_i \equiv \varphi(x_i)$ and $D_{ij}^{-1} \equiv D^{-1}(x_i - x_j)$, see Eq. (10). In the last step, we inserted the free action of Eq. (9) and the field-theory generalization of Eq. (7). Also in this case, we can visualize the r.h.s. of Eq. (11) by the diagrams shown in Fig. 4, for $i, j, k, l = 1, 2, 3, 4$.

Now this is not really a “scattering” amplitude; after all, we have free fields which cannot scatter. Real scattering requires interaction, and it is only at this point where we need to make an approximation. Namely, we assume that the interaction is “small”. But small w.r.t. what? The answer to this question can, strictly speaking, only be given pragmatically and in retrospect: sufficiently small for the approximation to work. The approximation is systematic, in the sense that it formally identifies parametrically suppressed terms. If, in the final result, these turn out to be small w.r.t. to the leading terms, we have an indication that the approach works.

We know cases where this approximation, called *perturbation theory*, works extremely well. The anomalous magnetic moment of the electron is the prime example: the perturbative calculation agrees perfectly with the measurement, which is known with an accuracy of one part in a trillion (see, e.g., Ref. [20]). In other cases, such as low-energy quantum chromodynamics (QCD), perturbation theory is known to fail. And there are intermediate cases, of course.

Interaction terms are represented by monomials in the action which are higher than quadratic in the fields. Again schematically:

$$S[\varphi] = -\int \mathrm{d}^4 x \left[\frac{1}{2} \varphi(x) D_x \varphi(x) - \frac{\lambda}{3!} \varphi^3(x) \right] \,. \tag{12}$$

[5] The expert reader will notice that we neglect the “$i\varepsilon$ prescription” in the propagators; it is irrelevant for our discussion. For details, see Ref. [19], for example.

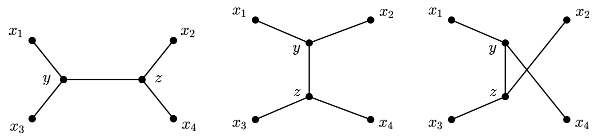

Fig. 5 Diagrams of order λ^2 for the four-point function.

$$\int \mathcal{D}\varphi\, \varphi\varphi \cdots \varphi \, \exp\left(iS[\varphi]\right) \quad \Rightarrow \quad D^{-1}D^{-1}\cdots \quad \Leftrightarrow$$

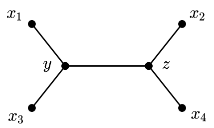

$$+\cdots$$

Fig. 6 From path integrals to propagators to Feynman diagrams, and back to propagators.

Assuming that λ is "sufficiently small", we may expand the exponential in the path integral and obtain the *perturbative series*

$$\begin{aligned} &\int \mathcal{D}\varphi \, \exp\left[-\frac{i}{2}\int \mathrm{d}^4x \left(\frac{1}{2}\varphi(x) D_x \varphi(x) - \frac{\lambda}{3!}\varphi^3(x)\right)\right] = \\ &= \int \mathcal{D}\varphi\, \exp\left(-\frac{i}{2}\int \mathrm{d}^4x\, \varphi(x) D_x \varphi(x)\right)\left[1 + \frac{\lambda}{3!}\int \mathrm{d}^4y\, \varphi^3(y)\right. \\ &\qquad \left. + \frac{1}{2}\left(\frac{\lambda}{3!}\right)^2 \int \mathrm{d}^4y\, \varphi^3(y) \int \mathrm{d}^4z\, \varphi^3(z) + \mathcal{O}(\lambda^3)\right]. \end{aligned} \tag{13}$$

Let us evaluate the four-point function with this action. The term of order λ^0 reproduces the result of Eq. (11) for the free theory, as one would expect. The order-λ term leads to a path integral with an odd number of fields φ, which vanishes due to the asymmetry of the integrand, see the discussion after Eq. (6). So the next non-zero term is of order λ^2. We can represent it again graphically, see Fig. 5. The *vertices* labeled y and z arise from the interaction. They involve three lines, corresponding to the three factors of $\varphi(y)$ and $\varphi(z)$ in the last line of Eq. (13). While $x_1, \ldots, x_4$ denote fixed physical space-time points, the location of the interaction points y and z is integrated over all space-time. Note that interchanging y and z thus does not lead to new diagrams, because it is merely a change of integration variables.[6]

4 Feynman diagrams

Applying perturbation theory was a crucial step in evaluating the path integral. It turns all occurring integrals into the Gaussian form, thus making their

[6] Aside from Fig. 12, one can also draw *disconnected* diagrams. It turns out that they can be disregarded though [19]).

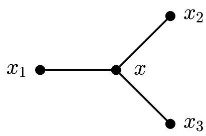

Fig. 7 Leading-order diagram for the three-point function.

evaluation trivial by applying well-known formulas (see Eq. (7)). The individual terms in the perturbative expansion can be represented diagrammatically. But this level of simplification is nothing special, because perturbation theory is a well-known approximation also in other contexts, which expresses physical quantities of a general interacting theory on the basis of the free theory.

But the considerations above lead us to a much more powerful conclusion, which is one of the central messages that we are trying to convey with this article (see also Fig. 6):

Diagrams like those of Fig. 5 not only visualize the individual terms of the perturbation series; one can actually construct the series from these diagrams, without ever having to use to path integral anymore.

For example, let us consider the three-point function,

$$\langle\varphi(x_1)\varphi(x_2)\varphi(x_3)\rangle\,. \tag{14}$$

At $\mathcal{O}(\lambda^0)$, there is no way we can connect three arbitrary points by a single line, which is consistent with the fact that the path integral over the free action with an odd power of integration variables vanishes by symmetry arguments. However, at $\mathcal{O}(\lambda)$, we need to incorporate one vertex, and we actually find the diagram shown in Fig. 7, which we may immediately translate into the expression

$$\lambda\int \mathrm{d}^4y\, D^{-1}(x_1-y)D^{-1}(x_2-y)D^{-1}(x_3-y)\,, \tag{15}$$

using the *Feynman rules* listed in the first and second column of Table 1.[7] No reference to the path integral is required to obtain this expression. In fact, not even the Lagrangian is needed: all the relevant information is contained in the Feynman rules. We see that the underlying particle model, including the intricacies of its QFT framework, is encoded in the Feynman diagrams and the associated Feynman rules of Table 1. Carrying it to the extreme, one might say that there is no more need for a practitioner to learn the concepts of QFT. Adopting the rules of Feynman diagrams is sufficient to make arbitrarily precise predictions for processes at particle colliders.

Recall, however, that one of the crucial ingredients to derive Feynman diagrams was perturbation theory. Therefore, they strictly apply only to cases

[7] The factor 1/3! in Eq. (13) cancels against the possibilities to connect the tree lines of the vertex with x_1, x_2 and x_3.

Table 1 Feynman rules for the spin-0 φ^3-theory in position (x) and momentum (p) space.

topology	x-space	p-space
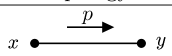	$D^{-1}(x,y)$	$\frac{i}{p^2-m^2}$
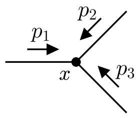	$\lambda\int \mathrm{d}^4x$	$\lambda\int \mathrm{d}^4p_3\delta^{(4)}(p_1+p_2+p_3)$

where the perturbative series converges (or is at least asymptotic). Nevertheless, the apparent conceptual distance between Feynman diagrams and the original quantum theory, as well as their theoretical autonomy may indicate that there is more behind Feynman diagrams than their derivation from QFT suggests. Most famously, such ideas gave rise to the so-called S-matrix program in the 1960s, by which it was argued that Feynman diagrams actually signal the existence of a theory that goes *beyond* QFT (see Ref. [8]).

Let us come back to the expression in Eq. (15) and insert Eq. (10) for the D^{-1}. One finds that the integration over y can be carried out immediately:

$$\begin{aligned}&\int \mathrm{d}^4y \exp\left[ip_1\cdot(x_1-y)\right]\,\exp\left[ip_2\cdot(x_2-y)\right]\,\exp\left[ip_3\cdot(x_3-y)\right]\\&=(2\pi)^4\exp\left[ip_1\cdot x_1\right]\,\exp\left[ip_2\cdot x_2\right]\,\exp\left[ip_3\cdot x_3\right]\delta^{(4)}(p_1+p_2+p_3)\,.\end{aligned}\tag{16}$$

Therefore, the mathematical expressions simplify considerably if we express them in momentum space. All that amounts to is to associate each line with a factor $\tilde{D}^{-1}$ instead of D^{-1}, see Eq. (10), and to enforce momentum conservation at each vertex, as implied by the δ-function in Eq. (16). This leads to the third column of Table 1. Thus, the diagram of Fig. 7 gives

$$\lambda\cdot\frac{i}{p_1^2-m^2}\cdot\frac{i}{p_2^2-m^2}\cdot\frac{i}{(p_1+p_2)^2-m^2}\,.\tag{17}$$

If we insert numerical values for the coupling λ, the momenta p_1 and p_2, and the mass m, all we get is a single complex number. We have come down the road from field operators and infinite-dimensional integrals, and arrived at a single number. Once the Feynman rules had been established, it was no longer necessary to refer to the path integral. The result was obtained by drawing a diagram and associating mathematical factors with each of its lines and vertices. These are arguably simple operations compared to the general evaluation of a multi-dimensional integral. But it is not even the full story. After all, the procedure is *algorithmic*, which means that by following a strict recipe, one arrives at the correct result. All intellectual effort has been absorbed by the algorithm which can be implemented in a computer program. At this level, the result can be obtained by "pressing a button". It is hard to imagine any simpler action than that.

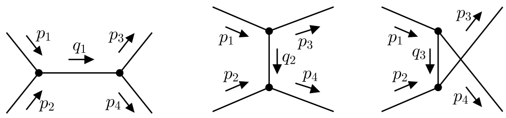

Fig. 8 Diagrams of order λ^2 for the $2 \to 2$ scattering amplitude. Note the differences to Fig. 5: while there the diagrams are understood in position space, here they are in momentum space. Also, the external propagators are removed, indicated by removing the dots at the ends. The diagrams are in one-to-one correspondence to the three terms of Eq. (18), which is why one refers to them as s-, t-, and u-channel, respectively.

Remember that the expression in Eq. (17) arose from particles associated with well-defined space-time points x_1, x_2, x_3. The quantities to be measured in experiment are scattering cross sections though, describing the probability for the transition of a quasi-free initial state at $t = -\infty$, to another, also quasi-free final state at $t = +\infty$. The interaction happens during a finite time interval in between. The theory for turning the initial and final states to such quasi-free states at $t = \pm\infty$ is quite involved and goes by the name of the LSZ-theorem [21, 22]. The upshot is just to remove the respective propagator $\tilde{D}^{-1}$ for each external particle and to replace it by its momentum-space wave function $\psi(p)$; for a spin-0 particle, this is just a constant $\psi(p) \sim 1$, for example. This provides one with the scattering amplitude $\mathcal{A}$, sometimes also referred to as the *Feynman amplitude*. It is the analogue of the probability amplitude introduced in Eq. (1), but rather than describing the transition between two space-time points, it relates the initial and final state of the scattering process to one another. The square of the Feynman amplitude can be interpreted as the probability density for the transition of a set of initial-state into a set of final-state particles, all with well-defined momenta. All that is left to turn this into a cross section are operations on the kinematical parameters: integration over the final-state phase space, and normalization by the initial flux (for details, see Ref. [19], for example).

Let us derive the Feynman amplitude for the elastic scattering of two particles with momenta p_1 and p_2 into p_3 and p_4. The relevant leading-order Feynman diagrams are shown in Fig. 5. In momentum space, and with the external propagators removed, one would draw them as in Fig. 8 though. The Feynman amplitude is given by the sum of the three diagrams:

$$\mathcal{A}_{\varphi\varphi\to\varphi\varphi} \sim \frac{1}{s - m^2} + \frac{1}{t - m^2} + \frac{1}{u - m^2}\,, \tag{18}$$

where (t is not to be confused with the time variable here)

$$s = q_1^2 = (p_1 + p_2)^2\,, \quad t = q_2^2 = (p_1 - p_3)^2\,, \quad u = q_3^2 = (p_1 - p_4)^2\,. \tag{19}$$

If we consider the process in the center-of-mass frame, then the four-momenta of the incoming particles take the values

$$p_1 = (E/2, \vec{p})\,, \qquad p_2 = (E/2, -\vec{p})\,, \tag{20}$$

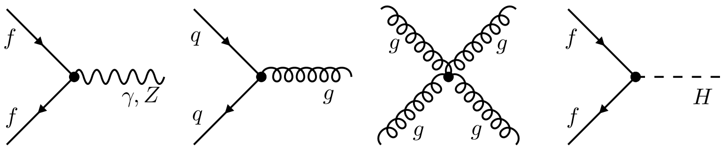

Fig. 9 A subset of the Feynman rules for the Standard Model. f denotes any charged fermion (lepton or quark), while q could be any quark. g is a gluon, and H the Higgs boson. Only the *topological part* (which particles couple to one another) of the Feynman rules is shown; the full set including the mathematical expressions can be found in Ref. [23], for example.

where $E = 2\sqrt{m^2 + \vec{p}^2}$. Therefore $s = E^2$, which means that if we adjust the center-of-mass energy to $E = m$, then the first term in the amplitude of Eq. (18) is divergent! While the actual divergence is cured by including higher orders of the perturbative series, it still leaves a significant enhancement around $s = m^2$, or in other words: a peak. We will see its implications in the next section.

5 Comparison to experiment

The preceding section was concerned with the reduction of the pragmatic complexity by introducing Feynman diagrams when deriving a physical quantity from the Lagrangian. In this section, we will argue that the correspondence between the structure of Feynman diagrams and experimental observation also introduces a remarkable epistemic simplification of QFT. This is because certain characteristics of experimental data, for example peaks in kinematical distributions, are directly related to specific features of Feynman diagrams, such as intermediate (*virtual*) particles.

So far, we have considered one of the simplest field theories, consisting of a single, uncharged particle φ. Nevertheless, the basic principles remain the same also in more realistic theories. The main difference is that we must introduce a separate field for each of the known particles: electron, photon, muon, neutrinos, quarks, gluons, etc. In Feynman diagrams, the lines associated with these particles need to be distinguished, for example by labeling them by the particle name, or a suitable short-hand notation (e for electron, μ for muon, γ for photon, etc.). In addition, one typically introduces different line styles for fermions, gauge bosons, and scalar particles.

What makes a theory, however, are not just the particles it contains, but also the interactions among them. Recall that interactions are encoded in the Lagrangian by products of three or more fields, cf. Eq. (12). For the simple theory above, we found that we can evaluate scattering amplitudes from the knowledge of the Feynman rules, without ever referring to the path integral or the Lagrangian. This is also the case for the Standard Model or any other particle model. All we need to do is to define the Feynman rules in analogy to

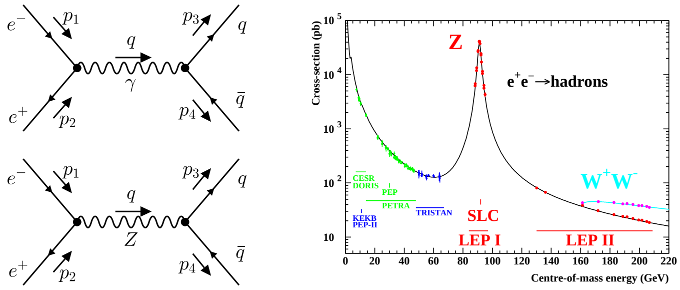

(a) (b)

Fig. 10 (a) Feynman diagrams contributing to the amplitude for the process of electron-positron annihilation into a quark/anti-quark pair, $e^+e^- \to q\bar{q}$, at leading order in perturbation theory. (b) Measured cross section [25].

Table 1: which particles couple to one another, and what is the corresponding mathematical term. As stated before: Feynman diagrams and the associated Feynman rules not only serve as a tool to do calculations within a particle model. They actually *encode* the particle model, including its QFT character.

A selection of the Standard Model Feynman rules is shown in Fig. 9; the full set is implemented in the program `FeynGame` [24].[8]

Note that not all fields of the Standard Model couple to one another in the Feynman rules. For example, while there are interaction terms involving two electrons and one photon in the Standard Model Lagrangian, products of three photons or three electrons are absent. Which terms are allowed and which are not is determined by the symmetries of the theory. Aside from Lorentz invariance (or, more general, Poincaré symmetry), the Standard Model is based on so-called gauge symmetries that go by the name of SU(3), SU(2), and U(1). Their precise meaning goes beyond the scope of this article though.

Given these rules, constructing the Feynman diagrams that lead to the amplitude for a realistic process is as easy as playing with LEGO®. We recommend the readers to try it out themselves: download `FeynGame` on your computer and start playing!

The graphical character of the Feynman diagrams thus implies an enormous pragmatic simplification when calculating particle reactions. All the terms of the perturbative expansion can be written down by following a set of graphical rules. But the simplification also has a significant epistemic character. To see this, let us consider the process $e^+e^- \to q\bar{q}$, which was one of the most important reactions at LEP, the predecessor of the Large Hadron Collider (LHC) at CERN. At leading order, using the $ff\gamma$ and ffZ vertices of Fig. 9 with $f = e$ and $f = q$, one arrives at the diagrams shown in Fig. 10 (a). Note that only s-channel diagrams contribute here (cf. Fig. 8), and the amplitude

[8] `FeynGame` was also used to draw all the diagrams in this article. It can be downloaded from `http://www.robert-harlander.de/software/feyngame`.

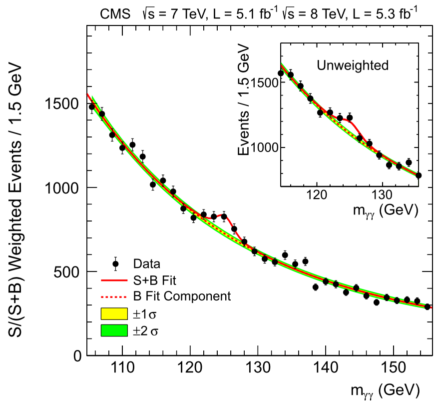

Fig. 11 The first observation of the Higgs boson by the CMS collaboration [26].

is proportional to

$$\mathcal{A}_{e^+e^-\to q\bar{q}} \sim \frac{i}{s} + C\,\frac{i}{s - M_Z^2}\,, \tag{21}$$

where C is a constant. The cross section should thus exhibit peaks around $\sqrt{s} = 0$ (the photon mass) and $\sqrt{s} \sim M_Z$ (the Z boson mass). Indeed this is what is observed experimentally, see Fig. 10 (b). Recall that the Feynman diagrams arose as graphical representations of the perturbative expansion, and that the diagrams shown in Fig. 10 (a) only represent the leading term of this series. Nevertheless, this peculiar behavior of the cross section somewhat suggests that the Z boson (and the photon, or their respective quantum fields) does play a special role in this process. Even though it leaves no physical track in the detector, the peak signals the existence of the Z boson. In fact, the "discovery" of the Higgs boson was actually the discovery of exactly such a peak in the cross section—albeit a much fainter one, see Fig. 11.

As if the enormous facilitation when calculating cross sections was not enough for praising Feynman diagrams, we now see that they even suggest an extremely intuitive picture(!) for what "actually" happens in a scattering reaction—so intuitive indeed that one easily runs the danger of overinterpretation. The question to what extent Feynman diagrams represent a physical process is clearly very interesting from a philosophical as well as a historical perspective. Feynman himself, for example, very much supported their positive ontological reading, while Dyson seemed to be more skeptical about this. Today, philosophers are still divided about this question (for two examples from opposite camps, see Refs. [27] and [28]).

Physicists, on the other hand, are typically quite pragmatic in this respect. A priori, Feynman diagrams are graphical representations of mathematical expressions. Their form is obviously very suggestive for reading them in terms of "(virtual) particle exchange", possibly even in a space-time picture (as Feynman does in his original paper [16]). With some experience, such language is very helpful in certain situations, as illustrated by the example of the Z boson "exchange" and the related peak in the cross section. Similarly, experts can associate certain divergences in scattering amplitudes to some line of a Feynman diagram "splitting collinearly into two", or "getting close to its mass shell" (i.e., the 4-momentum p approaches $p^2 = m^2$, with m the mass of the associated particle).

The possibility of reading Feynman diagrams in this way means a significant epistemic simplification, since the ostensiveness helps to understand the interrelations of QFT, as also argued in Ref. [13]. For this to work, it is not necessary to assign any reality status to the lines of the diagram. We strictly associate the Z-line in Fig. 10 (a) only with the occurrence of the peak at $\sqrt{s} \approx M_Z$, *not* with the presence of a physical particle at any point in time. After all, quantum physics is quite clear about what one can know about a system, and what not. And the question of whether a particle is exchanged or not in a scattering reaction is of the same quality as the question about which slit the particle traversed in the double-slit experiment of Fig. 2: it simply has no answer in quantum mechanics—not even a probabilistic one.[9] But in the same way as it is helpful to think in terms of a particle traversing the slits of Fig. 2 (a) along the classical paths in order to compute the probability distribution, it is helpful to adopt this quasi-classical way of thinking about Feynman diagrams.

6 Higher orders in perturbation theory

Now that we have learned about all the virtues of Feynman diagrams, it is time to bring ourselves back down to earth. Remember once again that the Feynman diagrams shown in Fig. 8 and Fig. 10 represent but the very first term in the perturbative series. Basing our theoretical prediction entirely on this leading-order term may be quite inaccurate. In fact, if we only know this term, we do not even have a good idea about the theoretical uncertainty induced by dropping all the higher order terms in the perturbative series.

Let us thus try to improve our prediction and supplement the $\mathcal{O}(\lambda^2)$ diagrams of Fig. 8 by those of order λ^4. Since each vertex contributes one power of λ, these diagrams must have four vertices, while the number of external legs remains the same as in Fig. 8, i.e. also four. The only way to achieve this is to introduce closed loops, and we arrive at the diagrams show in Fig. 12. Obviously, there are quite a bit more of them than at $\mathcal{O}(\lambda^2)$. And this is already the first complication when going to higher orders: the number of diagrams roughly increases factorially with the order of perturbation theory. In current calculations it is no exception that the number of diagrams to be evaluated is of the order of a million.

[9] That is to say that an answer to this question requires a certain level of *interpretation* of quantum mechanics which is a subject that we are not going to address here (see, e.g., Ref. [1]).

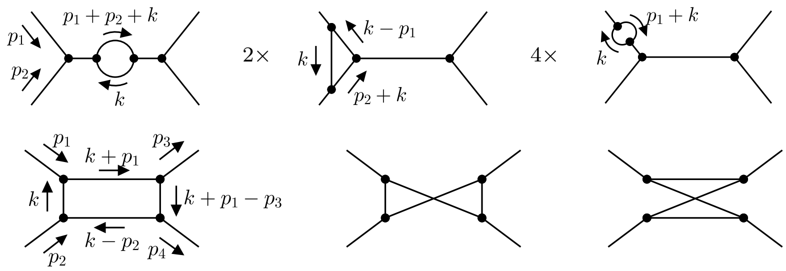

Fig. 12 One-loop diagrams contributing to 2 → 2 scattering at $\mathcal{O}(\lambda^4)$. The factors in front of some diagrams indicate the number of similar diagrams which are not shown. For each of the diagrams in the upper row, there are two more analogous ones derived from the leading-order diagrams, see Fig. 8. So in total, there are $3(1+2+4)+3=24$ one-loop diagrams. The momentum k is not determined by the external momenta $p_1,\ldots,p_4$. It is the so-called loop-momentum and needs to be integrated over. Only exemplary momentum assignments are shown.

But, as we outlined above, the generation of Feynman diagrams is a strictly algorithmic task to all orders in perturbation theory. It can thus be handed over to a computer and considered as solved for all practical purposes. Note that at this point we have switched from “drawing” the diagrams to their “generation”. The actual *images* of the diagrams are skipped over in modern perturbative calculations. We will come back to this aspect in Section 7.

The number of diagrams is only one aspect though. A second problem of higher-order calculations becomes clear when assigning momenta to the lines of a loop diagram: momentum conservation at the vertices is not sufficient to uniquely express the momenta of loop lines in terms of the external momenta. In Fig. 12, the “loop momentum” is denoted by k; the reader may verify that momentum conservation at the vertices holds for any value of k.

This implies that each closed loop introduces a four-dimensional momentum integration $\int \mathrm{d}^4k$. Since integration is *not* an algorithmic process in general, higher-order calculations typically require additional intellectual efforts. Nevertheless, the integrals which occur in perturbative calculations of QFT are of a very particular form, so one may try to develop further algorithms for their evaluation. Indeed, in the one-loop case, the problem is solved in full generality. Starting from two loops, however, only specific kinematical configurations can be calculated with current technology. For very special cases, one has reached the five-loop level, but that is currently about as good as it gets.

Still, the calculation of *loop integrals* is a field of continuous progress. Most efforts go into the construction of algorithms which map integrals of a certain class to a relatively small set of so-called *master integrals*. The most important algorithms in this respect are *tensor reduction* [29] and *integration-by-parts* [30], with a number of significant refinements and additions (see, e.g., Refs. [31, 32]).

But at some point, one needs to face the facts and evaluate the master integrals. One of the main difficulties here is that the loop integrals are divergent in general, i.e., strictly speaking: undefined. The way how one can still make *physical* sense of this is beyond the scope of this article; it was recognized by a Nobel prize to Feynman, Schwinger, and Tomonaga in 1965. But even leaving the physical interpretation aside, one has the problem of making *mathematical* sense of these divergent integrals. One of the early breakthroughs in this respect was the development of *dimensional regularization* [33], where one continues the four-dimensional integration volume to $d = 4 - 2\epsilon$ dimensions. This isolates the divergences as poles at $\epsilon \to 0$. Obviously, dealing with non-integer (actually complex-valued!) dimensions leads to other technical challenges, and also here physicists have made continuous progress in order to keep up with the ever increasing experimental precision (see Ref. [34], for example).

Finally, it turns out that the loop integrals often cannot be expressed in terms of known mathematical functions. Physicists have thus come up with whole new classes of functions, such as Harmonic Polylogarithms [35]. In this way, physics remains one of the driving fields for applied mathematics.

7 Feynman diagrams in present-day calculations

The various uses of Feynman diagrams in everyday and professional *communication* by physicists has been discussed in Refs. [8, 10], for example. In this respect, it is obviously crucial that they allow to convey a lot of information by simply drawing a few lines on a piece of paper or a blackboard. Historically, the visual aspect certainly also played an important role in the actual *calculation* of scattering and decay processes. After some practice, it becomes rather intuitive to generate all terms that contribute to, say, the leading or maybe next-to-leading order in perturbation theory by simply drawing the relevant diagrams. This is the pragmatic aspect of simplification due to the graphical nature of the diagrams discussed in Section 5.

In present-day calculations, however, we have long arrived at a point where the visual aspect of the diagrams in perturbative calculations has moved to the background. In the ideal case, no human ever needs to look at the diagrams any more, as we will describe in the following. It will be useful in this section to follow the mathematical custom and distinguish a *graph*, which contains the abstract topological information (i.e. which line, or *edge*, is connected to which of the vertices), from a *diagram*, which is the visual representation of a graph. In other words, if one literally *draws* all the lines and vertices of a graph, one obtains a diagram.

Let us now consider a typical modern setup for the calculation of a process at higher orders in perturbation theory. The particle model (recall footnote 1) is encoded in terms of the Feynman rules, as given by the left and the right column in Table 1. We will refer to the left column of this table as the *topological* part of a Feynman rule (which particles are connected by a vertex), and to the right column as the *mathematical* part (what is the mathematical expression

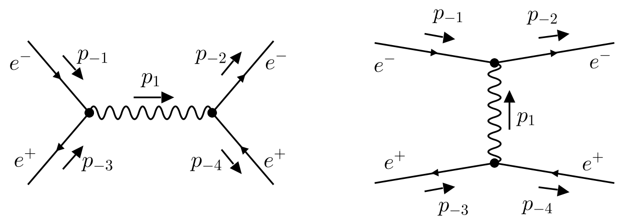

Fig. 13 The two tree-level diagrams for the process $e^+e^- \to e^+e^-$ in QED. Their `qgraf` encoding is shown in Listing 2.

corresponding to the specific vertex or propagator). Adopting the notation of `qgraf` [36, 37] which is one of the most efficient Feynman graph generators, the topological part of the Feynman rules for quantum electrodynamics (QED) can be defined as

```
1 [fq,fQ,-]
2 [a,a,+]
3 [fQ,fq,a]
```

Listing 1 QED in `qgraf` notation.

where the first two lines encode the relevant properties of the electron and the photon, respectively. The first entry inside the square bracket denotes the particle (`fq`$\hat{=}e^-$, `a`$\hat{=}\gamma$), the second one its anti-particle (`fQ`$\hat{=}e^+$; the photon and its anti-particle are identical), and the third entry indicates whether the particle obeys fermionic or bosonic statistics (`-` or `+`). The third line in Listing 1 defines the interaction term of the left-most vertex in Fig. 9 (taking only into account the photon γ). This information is sufficient to generate all Feynman graphs for any given initial and final state up to arbitrary[10] loop order, including the relevant signs and symmetry factors.

At tree-level, the output of `qgraf` for the process $e^+e^- \to e^+e^-$ reads:

```
*--#[ d1:
*
     1
    *vx(fQ(-3),fq(-1),a(1))
    *vx(fQ(-2),fq(-4),a(1))
*
*--#] d1:
*--#[ d2:
*
     -1
    *vx(fQ(-2),fq(-1),a(1))
    *vx(fQ(-3),fq(-4),a(1))
*
*--#] d2:
```

Listing 2 The graphs of Fig. 13 in `qgraf` notation.

[10] Limitations are set only due to the available hardware resources.

Here, `vx(...)` denotes a vertex, and the integers label lines of the Feynman graph. Negative integers label incoming (odd) and outgoing (even) particles. The corresponding Feynman diagrams, i.e. the visual representation of these graphs, is shown in Fig. 13. Now one can simply ask `qgraf` to generate higher-order graphs for this process. At one-, two-, three-, and four-loop level, this leads to 18, 186, 2264, and 31860 graphs, respectively. It takes `qgraf` less than two seconds to produce this output. Below is an example for a three-loop graph:

```
*--#[ d1437:
*
     1
    *vx(fQ(-3),fq(2),a(1))
    *vx(fQ(3),fq(-4),a(1))
    *vx(fQ(-2),fq(5),a(4))
    *vx(fQ(7),fq(-1),a(6))
    *vx(fQ(2),fq(8),a(4))
    *vx(fQ(9),fq(3),a(6))
    *vx(fQ(5),fq(9),a(10))
    *vx(fQ(8),fq(7),a(10))
*
*--#] d1437:
```

Listing 3 A three-loop graph for the process $e^+e^- \to e^+e^-$ in QED in `qgraf` notation.

Obviously, it is quite an effort for a human to visualize this expression in terms of a diagram (the reader is encouraged to try this; `FeynGame` can be very helpful here). Of course, it is possible to automate also the visualization,[11] but who would want to look at (hundreds of) thousands of diagrams, and what would that be good for anyway? Despite the suggestive character of these questions, the answer is not plainly “nobody” and “nothing”, as we will see further below.

The computer simply uses the topological information above to route the external and the loop momenta through the graph, taking into account momentum conservation at each vertex. For example, while the momentum of line 1 in the left diagram of Fig. 13 is $p_1 = p_{-1} + p_{-3}$, it is $p_1 = p_{-2} - p_{-1}$ in the right diagram. With this information, it generates a mathematical expression by using the mathematical part of the Feynman rule for each of the lines and vertices (i.e., inserting expressions like those in the right column of Table 1). At this point, the graphs have done their duty, and the problem has turned into a purely mathematical one. And it is from this step onward where most of the current efforts in perturbative calculations go, see Section 6. Ideally, the computer will now apply further algorithms to perform the required algebraic or numerical operations until it arrives at the *bare* result for the scattering or decay amplitude under consideration. The next step is renormalization, which in principle can be automated as well.

It is important to note that what we have just described is the ideal case for this kind of perturbation calculations. In the development phase of a particular

[11] See Ref. [38], for example. While such kind of visualization is straightforward in principle, it turns out to be incomparably more difficult to turn the diagram into a form which is most pleasing to the human eye.

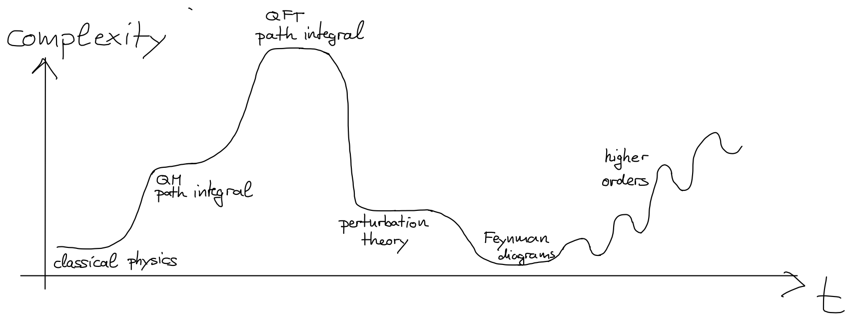

Fig. 14 Schematic representation of the ups and downs of complexity on the way from classical physics to quantitative predictions in particle physics.

software tool or calculation, the workflow will usually break down or get stuck at some point. It is in this debugging or trimming phase where the visual aspect of Feynman diagrams still plays a role in present-day calculations. Every so often, the automatic setup will work up to, say, graph number 23612, where suddenly the automated calculation either terminates or stalls (e.g., no further output is logged while the CPU is fully loaded). One of the first items on the action list in this case is to *look* at that diagram, i.e. to reconstruct the visual representation from the topological code of the graph as the one in Listing 3. Quite often, this will immediately reveal the source of the problems: Does it contain a particle or vertex whose Feynman rule we missed to implement? Does the structure of the diagram reveal a potential singularity which prevents the convergence of the numerical integration? It may also happen that the calculation runs through, but the result is obviously wrong: it is not finite after renormalization, or it is gauge dependent, etc. Then it may help to skim through the whole catalog of diagrams by eye, to see if one notices something like a whole missing class of diagrams (no four-gluon vertices, no ghosts, etc.). Or one searches for two diagrams which are topologically related by, say, a mirror symmetry, and for which one knows that they must yield the same result. If they do not, this will also help to hunt down the bug.

Let us add that this pragmatic aspect is just one example for uses of (the visual dimension of) Feynman diagrams in today's calculations. Another one is related to the epistemic aspect discussed in Section 5, namely the identification of the analytic structure of a particular perturbative quantity: where are the kinematic singularities, where are branch cuts, etc.? An exhaustive collection and characterization of such applications is beyond the scope of this paper and shall be left for future investigation.

8 Conclusions

I have tried to sketch the central steps from the path integral to Feynman diagrams. Of course, this has been a rather ambitious endeavor, considering the fact that this required to summarize several years of material of academic studies of physics in a few pages. On the other hand, the purpose of this article has not been to provide a comprehensive pedagogical treatment. Rather, I wanted to show the dialectics behind Feynman diagrams. How, on the one hand, they manage to boil down the incredibly complex structure of QFT by destilling and transforming the relevant information into an algorithmic, stand-alone set of rules. One way to appreciate this even more is to consider the enormous technical efforts that are required in some alternative approaches to solving the path integral, above all lattice gauge theory. And yet, on the other hand, the quest for ever higher precision has led to an increase in complexity in practical applications, necessitating the need to develop further algorithms, mostly for the evaluation of the occurring integrals. Fig. 14 is meant to qualitatively illustrate this up-and-down in complexity.

Nevertheless, in my personal opinion, we may be approaching a point where Feynman diagrams (or graphs) have done their bit, in particular if evidence for physics beyond the Standard Model continues to elude the LHC. Sooner or later, we will come up with a new way to compare theory and experiment without the need for calculating millions of Feynman diagrams. This may then lead to the next valley in Fig. 14. Every now and then, a new idea in this direction pops up, but so far none of them has managed to significantly reduce the use of Feynman diagrams. Among the more use-oriented approaches are recursive techniques which cover whole groups of Feynman diagrams. Early works in this direction were simply aimed for a more efficient calculation of such amplitudes [39, 40], while later research led to a deeper understanding of the underlying relations among amplitudes (see, e.g., Refs. [41–43]). A more radical attempt is the *amplituhedron* [44], for example, but it still seems rather detached from an application to calculations within the Standard Model. So far, most of the results within this method have been restricted to academic theories with a large number of symmetries ($N = 4$ super-Yang-Mills). Another observation is that machine learning, which has become abound in almost all fields of academic, commercial, and everyday life, has also found its way into the field of perturbative calculations. One could imagine that a break-through will be achieved from this direction as well.

Either way, I am sure that the era of Feynman diagrams will be remembered as a successful one for the development of fundamental physics.

References

1. J. Ismael, *Quantum Mechanics* in: Edward N. Zalta, *The Stanford Encyclopedia of Philosophy* (2020), Metaphysics Research Lab, Stanford University, `https://plato.stanford.edu/archives/win2020/entries/qm/`

2. M. Kuhlmann, *Quantum Field Theory* in: Edward N. Zalta, *The Stanford Encyclopedia of Philosophy* (2020), Metaphysics Research Lab, Stanford University, `https://plato.stanford.edu/archives/fall2020/entries/quantum-field-theory/`
3. R. Frigg and S. Hartmann, *Models in Science* in: Edward N. Zalta, *The Stanford Encyclopedia of Philosophy* (2020), Metaphysics Research Lab, Stanford University, `https://plato.stanford.edu/archives/spr2020/entries/models-science/`
4. J.R. Brown, *How Do Feynman Diagrams Work?*, *Perspectives on Science* **26** (2018) 423.
5. M. Dorato and E. Rossanese, *The Nature of Representation in Feynman Diagrams*, *Perspectives on Science* **26** (2018) 443.
6. A. Wüthrich, *The Exigencies of War and the Stink of a Theoretical Problem: Understanding the Genesis of Feynman's Quantum Electrodynamics as Mechanistic Modelling at Different Levels*, *Perspectives on Science* **26** (2018) 501.
7. S.S. Schweber, *QED and the men who made it: Dyson, Feynman, Schwinger, and Tomonaga*, Princeton University Press, 1994.
8. D. Kaiser, *Drawing theories apart: The dispersion of Feynman diagrams in postwar physics*, University of Chicago Press, 1993.
9. A. Wüthrich, *The Genesis of Feynman Diagrams*, Springer, 2010.
10. M. Stöltzner, *Feynman Diagrams: Modeling between Physics and Mathematics*, *Perspectives on Science* **26** (2018) 482.
11. M. Bunge, *The Complexity of Simplicity*, *The Journal of Philosophy* **59** (1962) 113.
12. S. Schindler, *Theoretical Virtues in Science: Uncovering Reality through Theory*, Cambridge University Press, 2018.
13. L. Meynell, *Picturing Feynman Diagrams and the Epistemology of Understanding*, *Perspectives on Science* **26** (2018) 459.
14. O. Darrigol, *The magic of Feynman's QED: from field-less electrodynamics to the Feynman diagrams*, *The European Physical Journal H* **44** (2019) 349. `https://doi.org/10.1140/epjh/e2019-100025-2`
15. R.P. Feynman, *Space-time approach to nonrelativistic quantum mechanics*, *Rev. Mod. Phys.* **20** (1948) 367.
16. R.P. Feynman, *The Theory of positrons*, *Phys. Rev.* **76** (1949) 749.
17. R.P. Feynman, *Space-time approach to quantum electrodynamics*, *Phys. Rev.* **76** (1949) 769.
18. R.P. Feynman and A. Hibbs, *Quantum Mechanics and Path Integrals*, McGraw-Hill College, 1965.
19. M.E. Peskin and D.V. Schroeder, *An Introduction to quantum field theory*, Addison-Wesley, 1995.
20. F. Jegerlehner, *The anomalous magnetic moment of the muon*, Springer, 2017.
21. H. Lehmann, K. Symanzik, and W. Zimmermann, *On the formulation of quantized field theories*, *Nuovo Cim.* **1** (1955) 205.
22. H. Lehmann, K. Symanzik, and W. Zimmermann, *On the formulation of quantized field theories. II*, *Nuovo Cim.* **6** (1957) 319.
23. J.C. Romao and J.P. Silva, *A resource for signs and Feynman diagrams of the Standard Model*, *Int. J. Mod. Phys. A* **27** (2012) 1230025, `arXiv:1209.6213 [hep-ph]`.
24. R. Harlander, S. Klein, and M. Lipp, *FeynGame*, *Comp. Phys. Commun.* **256** (2020) 107465, `arXiv:2003.00896 [physics.ed-ph]`.
25. S. Schael *et al.*, *Precision electroweak measurements on the Z resonance*, *Physics Reports* **427** (2006) 257.
26. S. Chatrchyan *et al.*, *Observation of a New Boson at a Mass of 125 GeV with the CMS Experiment at the LHC*, *Phys. Lett. B* **716** (2012) 30, `arXiv:1207.7235 [hep-ex]`.
27. L. Meynell, *Why Feynman diagrams represent*, *Int. Stud. Phil. Sc.* **22** (2008) 39.
28. O. Passon, *On the interpretation of Feynman diagrams, or, did the LHC experiments observe $H \to \gamma\gamma$?*, *European Journal for Philosophy of Science* **9** (2019) 20.
29. G. Passarino and M. Veltman, *One loop corrections for e^+e^- annihilation into $\mu^+\mu^-$ in the Weinberg model*, *Nucl. Phys. B* **160** (1979) 151.
30. K.G. Chetyrkin and F.V. Tkachov, *Integration by parts: the algorithm to calculate beta functions in 4 loops*, *Nucl. Phys.* **B192** (1981) 159.
31. S. Laporta, *High precision calculation of multiloop Feynman integrals by difference equations*, *Int. J. Mod. Phys.* **A15** (2000) 5087, `hep-ph/0102033`.

32. J.M. Henn, *Multiloop integrals in dimensional regularization made simple*, *Phys. Rev. Lett.* **110** (2013) 251601, `arXiv:1304.1806 [hep-th]`.
33. G. 't Hooft and M. Veltman, *Regularization and Renormalization of Gauge Fields*, *Nucl. Phys. B* **44** (1972) 189.
34. T. Binoth and G. Heinrich, *Numerical evaluation of multiloop integrals by sector decomposition*, *Nucl. Phys.* **B680** (2004) 375, `hep-ph/0305234`.
35. E. Remiddi and J. Vermaseren, *Harmonic polylogarithms*, *Int. J. Mod. Phys. A* **15** (2000) 725, `hep-ph/9905237`.
36. P. Nogueira, *Automatic Feynman graph generation*, *J. Comput. Phys.* **105** (1993) 279.
37. P. Nogueira, *Abusing qgraf*, *Nucl. Instrum. Meth.* **A559** (2006) 220.
38. N. Deutschmann, *qgraf-xml-drawer*, `https://doi.org/10.5281/zenodo.164393`.
39. F.A. Berends and W.T. Giele, *Recursive Calculations for Processes with n Gluons*, *Nucl. Phys. B* **306** (1988) 759.
40. A. Kanaki and C.G. Papadopoulos, *HELAC: A Package to compute electroweak helicity amplitudes*, *Comput. Phys. Commun.* **132** (2000) 306, `hep-ph/0002082`.
41. E. Witten, *Perturbative gauge theory as a string theory in twistor space*, *Commun. Math. Phys.* **252** (2004) 189, `hep-th/0312171`.
42. R. Britto, F. Cachazo, B. Feng, and E. Witten, *Direct proof of tree-level recursion relation in Yang-Mills theory*, *Phys. Rev. Lett.* **94** (2005) 181602, `hep-th/0501052`.
43. Z. Bern, J.J.M. Carrasco, and H. Johansson, *New Relations for Gauge-Theory Amplitudes*, *Phys. Rev. D* **78** (2008) 085011, `arXiv:0805.3993 [hep-ph]`.
44. N. Arkani-Hamed and J. Trnka, *The Amplituhedron*, *JHEP* **10** (2014) 030, `arXiv:1312.2007 [hep-th]`.